Dyes and Pigments 95 (2012) 290–295

Contents lists available at SciVerse ScienceDirect

Dyes and Pigments

journal homepage: www.elsevier.com/locate/dyepig

C343 behavior in benzene/AOT reverse micelles. The role of the dye solubilization in the non-polar organic pseudophase

Jorge A. Gutierrez, R. Darío Falcone, Juana J. Silber, N. Mariano Correa*

Departamento de Química, Universidad Nacional de Río Cuarto, Agencia Postal # 3, (X5804ALH), 5800 Río Cuarto, Argentina

ARTICLE INFO

Article history:
Received 8 February 2012
Received in revised form
4 April 2012
Accepted 29 April 2012
Available online 11 May 2012

Keywords:
Coumarin C343
Reverse micelle
Micelar interface
Molecular probe
AOT
Hydrogen bond

ABSTRACT

The behavior of coumarin 343 (C343), a common molecular probe utilized in solvation dynamics experiments, was studied in water/sodium 1,4-bis-2-ethylhexylsulfosuccinate (AOT)/benzene reverse micelles (RMs). In all the studies performed until now, C343 was not soluble in the organic solvent used to create the RM systems (namely different alkanes such as *n*-heptane, cyclohexane or isooctane). In this work we have chosen benzene as the organic solvent because C343 is completely soluble at the work concentration used ($\sim 10^{-6}$ M). Thus, a well known AOT RM system: benzene/AOT/water has been used in order to gain insights, for the first time, on how the RMs' formation can affect the C343 spectroscopic behavior.

Dissolved in pure benzene C343 exists as a dimer since the intermolecular H-bond interactions are very strong in this solvent. When introduced to the AOT RMs, C343 resides in the RMs' interface and, at low occupation number the probability of finding more than one C343 molecule is reduced and only C343 monomer species is detected. From the spectral changes it was possible to determine the critical micelle concentration at $W_0 = 0$ and 10 and the C343 partition constants between two pseudophases.

In summary, in this work we have shown how the spectroscopic behavior of C343 is dramatically altered because of the partition of the dye to the AOT RMs' interfaces.

1. Introduction

The 7-aminocoumarins, such as coumarin 343, C343 (Scheme 1), are strong chromophores that are used in a broad range of applications such as laser dyes [1] and probing the dynamics of condensed-phase environments like solutions and in more complex environments like proteins and organized systems [2–10]. Basically, the properties that cause the 7-aminocoumarins to be effective for those purposes are (1) they are rigid, (2) they have strong radiative rates and (3) they possess strong solvatochromism [11].

It is already known that the absorption and emission spectroscopy of C343 depends strongly on its environment [12–17]. In this way, we have demonstrated [10] that polarity of the solvent (π^*) alone cannot account for the solvatochromic behavior of C343 and, that specific interactions play an important role in the C343 spectroscopy. Specifically, in the ground state the molecule displays a bathochromic shift with π^* and the H-bond acceptor (β) ability of the solvents. The carboxylic acid group causes C343 to display greater sensitivity to the β than to the π^* polarity parameter; this sensitivity increases in the excited state. This challenges the general interpretation of C343s solvatochromic behavior that primarily reflects the polarity of the medium [12,17]. Moreover, in that work it was demonstrated that due to its very low solubility, C343 forms a J-aggregate with non-defined stoichiometry in non-polar solvents or solvents with low polarity and H-bond acceptance ability [10].

Recently [18], we have shown the implications of the medium polarity, π^*, in the C343 inter/intramolecular H-bond interactions and the role that this interaction plays in the aggregation process of the dye. In pure benzene and because of the high C343 solubility, it has been postulated that the aggregate species is a dimer which prevails because the intermolecular H-bond interaction is favored. On the other hand, as the *n*-heptane content increases and the polarity of the mixture decreases, the intramolecular H-bond is the strongest and the C343 monomer is favored [18]. Thus, clearly the medium has a remarkable impact on C343 aggregation process.

Reverse micelles (RMs) are aggregates of surfactants formed in a non-polar solvent. The polar head groups of the surfactants point inward and the hydrocarbon chains point toward to the non-polar medium [19–21]. A common surfactant used to form RMs is sodium 1,4-bis (2- ethylhexyl) sulfosuccinate (AOT)

* Corresponding author. Fax: +54 358 4676233.
E-mail addresses: mcorrea@exa.unrc.edu.ar, nmcrio42004@yahoo.com.ar (N.M. Correa).

0143-7208/$ – see front matter © 2012 Elsevier Ltd. All rights reserved.
doi:10.1016/j.dyepig.2012.04.018

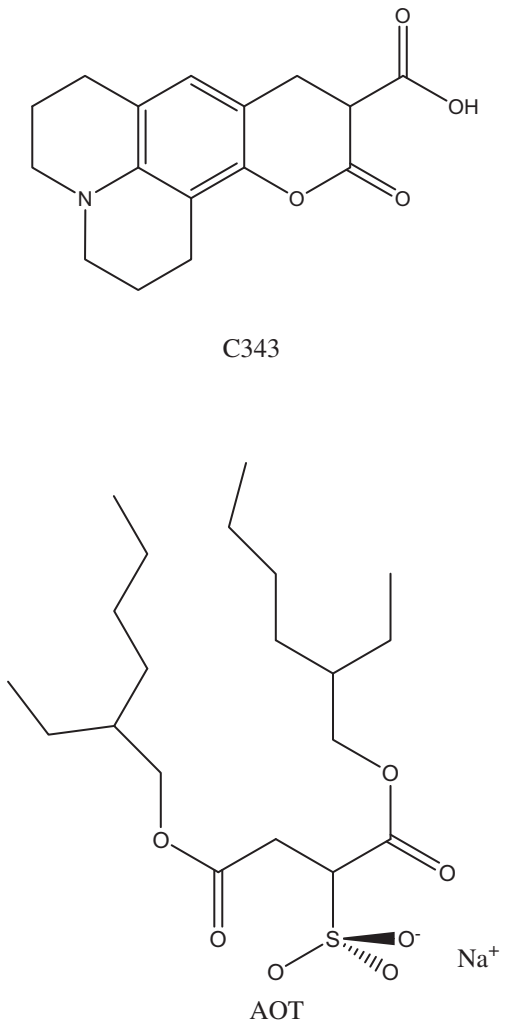

Scheme 1. Molecular structure of dye C343 and the surfactant AOT.

(Scheme 1). The RMs formed with this surfactant can solubilize a large quantity of water in a wide range of non-polar solvents, reaching values of $W_0 = [H_2O]/[AOT]$ as large as 40–60 depending on the non-polar solvent, the solute and the temperature [19–21]. RMs can be interesting microreactors for heterogeneous chemistry, as well as templates for nanoparticles and models for biological membranes [22].

Frequently and because of C343 has sensitivity to specific properties of the systems, it has been used to learn about the structure of different organized media such as RMs [2–6,17,23,24]. The use of C343 to monitor interesting RMs' properties has always been performed in RMs where C343 is not soluble in the organic pseudophase. In the majority of the studies, the non-polar organic solvents used were alkanes such as *n*-heptane, isooctane and cyclohexane where C343 solubility is negligible and the low solubility leads it to be located at micelle interfaces or interior avoiding problems of partitioning [2,3,9,10,17].

On the other hand, aromatic solvents such as benzene and toluene can also be used to create the RMs [19,25] and, as the C343 solubility is higher than in saturated hydrocarbons it can be investigated in the system even when RMs are not present. Very valuable information can be obtained if the molecular probe is dissolved in the non-polar pseudophase and the whole RMs' formation process is monitored. Therefore, critical micelle concentration (CMC), changes in the surrounding micropolarity and microviscosity and, how the external solvent can affect the water structure and interfacial properties upon encapsulation can be investigated. Moreover, RMs' media can dramatically affect molecular probe properties that cannot be possible to do when they are dissolved in homogeneous media, for example, acid–base and aggregation equilibriums [10,26,27].

Thus, in this work, we perform a detailed investigation about the C343 behavior in benzene/AOT/water RMs using absorption and emission spectroscopy at different surfactant and water concentrations. The aim of the work is to investigate how the partition process between benzene and AOT RMs can affect the spectroscopic behavior of C343. For this reason we have chosen a well-known AOT RMs' system: benzene/AOT/water [28–31] in order to gain insights on how the RMs' formation can affect the C343 spectroscopic behavior.

The results show that C343 dimer species in benzene is converted into monomer (de-aggregation process of the dye) when the AOT RMs is forming. Consequently, C343 exists solely as monomer at the RMs' interface at $W_0 = 0$ and 10. The dye de-aggregation process was used in order to evaluate the CMC of the RMs and, the spectral changes allow us to calculate C343 partition constant between two pseudophases. It seems that water molecules penetrate more into the oil side of the RMs' interface when benzene is the non-polar organic solvent as it was suggested previously [25,28–31].

2. Materials and methods

2.1. Materials

Sodium 1,4-bis (2-ethylhexyl) sulfosuccinate (AOT) (Sigma >99% purity) was used as received and was kept under vacuum over P_2O_5 to minimize H_2O absorption. The absence of acidic impurities was confirmed through the 1-methyl-8-oxyquinolinium betaine (QB) absorption bands [28].

Coumarin 343 (C343, Exciton) was used without further purification. Benzene (Merck spectroscopic quality) was used as received and ultrapure water was obtained from Labonco equipment model 90901-01.

2.2. Methods

The stock solutions of AOT in the benzene were prepared by mass and volumetric dilution. To obtain optically clear solutions they were shaken in a sonicating bath and, water was added using a calibrated microsyringe. The amount of water present in the system is expressed as the molar ratio between polar solvent and the surfactant ($W_0 = [H_2O]/[AOT]$) and was kept constant and equal to 0 or 10 in every system investigated.

To introduce the molecular probes, a 0.01 M solution of C343 was prepared in acetonitrile (Sintorgan HPLC quality). The appropriate amount of this solution to obtain a given concentration (6.0×10^{-6} M) of the probe in the micellar medium was transferred into a volumetric flask, and the acetonitrile was evaporated by bubbling dry N_2; then, the surfactant RMs' solution was added to the residue to obtain a [AOT] = 0.30 M. The stock solution of AOT 0.30 M and the molecular probe were agitated in a sonicating bath until the RMs were optically clear. To the cell baring 2 mL of C343 of the same concentration in the aromatic solvent, was added the appropriate amount of surfactant and molecular probe stock solution to obtain a given concentration of surfactant in the micellar media. Therefore, the absorption or emission of the molecular probe was not affected by dilution.

All experimental points were measured three times with different prepared samples. The pooled standard deviation was less than 5%. In all the cases, the temperature was kept at 25 °C ± 0.2 °C.

2.3. General

UV/visible spectra were recorded using a spectrophotometer Shimadzu 2401 with a thermostated sample holder. A Spex fluoromax apparatus was employed for the fluorescent measurements. Corrected fluorescence spectra were obtained using the correction file provided by the manufacturer. The path length used in the absorption and emission experiments was 1 cm. λ_{max} was measured by taking the midpoint between the two positions of the spectrum where the absorbance is equal to $0.90 \times A_{max}$. The uncertainties in λ_{max} are about 0.10 nm.

3. Results and discussions

3.1. C343 in benzene/AOT reverse micelles. $W_0 = 0$

Previous spectroscopic studies performed in cyclohexane reveal that due to its low solubility, C343 forms aggregates with no defined stoichiometry.[10] It seems that non-specific interactions (solvophobic interaction) play a key role to make the C343 aggregation process to go beyond the simple monomer–dimer equilibrium yielding higher-order aggregates. This conclusion was based on the absence of a clear isosbestic point in the C343 absorption spectra varying the dye concentration. The spectroscopic data showed that, in cyclohexane the monomer species absorbs at 405 nm and emits at 435 nm, while for the higher-order aggregates species the absorption band peaks at 425 nm and emits at 460 nm with low emission quantum yield in comparison with the monomer emission quantum yield [10]. On the other hand, and it was discussed above, in benzene C343 forms dimer species ($\lambda_{maxabs} = 442$ nm and $\lambda_{maxem} = 462$ nm) because the dye solubility is higher in comparison with cyclohexane and the inter H-bond interaction is favored with respect to the intra H-bond interaction [18].

Fig. 1 shows the absorption spectra of C343 in benzene/AOT RMs varying the surfactant concentration at $W_0 = 0$. As can be seen, in benzene the absorption spectrum has a maximum at $\lambda_{max} = 442$ nm and a shoulder at 421 nm that was previously assigned to the C343 dimer species [18]. As the AOT concentration increases, the absorbance of the low energy band decreases and a new band develops at $\lambda_{max} = 416$ nm which shifts to $\lambda_{max} = 409$ nm at AOT 0.30 M. Interestingly, the band that peaks at $\lambda_{max} = 442$ nm that correspond to the dimer species does not shift with the surfactant concentration, results that probably reflect the fact that C343 dimer is located only in the benzene pseudophase.

Moreover, it can be seen a clear isosbestic point at 421 nm that suggests the presence of two different species involved in a simple equilibrium. A question may arise here about which are the species and what is the nature of this equilibrium? As it was mentioned above, in previous work we found that in benzene at [C343] = 6×10^{-6} M, the dye forms J type dimer through intermolecular H-bond interaction between two C343 carboxyl groups (Scheme 1) with an absorption band at $\lambda = 442$ nm [18]. On the other hand, unlike its behavior in benzene, it is known that C343 does not aggregate in the RMs, which can be explained through Poissonian statistics [10]. At surfactant concentrations above the CMC, the occupation number is defined by Eq. (1):

$$n = \frac{[\text{dye}]}{[\text{RM}]} \tag{1}$$

where [RM] represents the concentration of RMs, defined by Eq. (2):

$$[\text{RM}] = \frac{[\text{Surfactant}] - \text{cmc}}{N_{agg}} \tag{2}$$

with N_{agg}, the aggregation number, that is the number of surfactant molecules in the RMs [32].

If on average, at the probe concentration used, $n < 1$, less than one molecule occupies any given RM and the environment leads to the complete de-aggregation of dye [10,33–35]. Thus, finding more than one dye molecule in any RM would be very unlikely and the aggregation process that C343 undergoes in benzene does not occur in the RMs' interface.

In summary, in pure benzene C343 exists as the dimer species with a $\lambda_{maxabs} = 442$ nm because the intermolecular H-bond interaction is favored, while in AOT RMs, C343 is located as monomer species at the interface with a $\lambda_{maxabs} = 409$ nm and the intramolecular H-bond is the strongest interaction.

Because C343 is more sensitive to the solvent polarity and the H-bond interaction in its excited state we used emission techniques to gain more insights about C343 behavior. Fig. 2 shows the emission

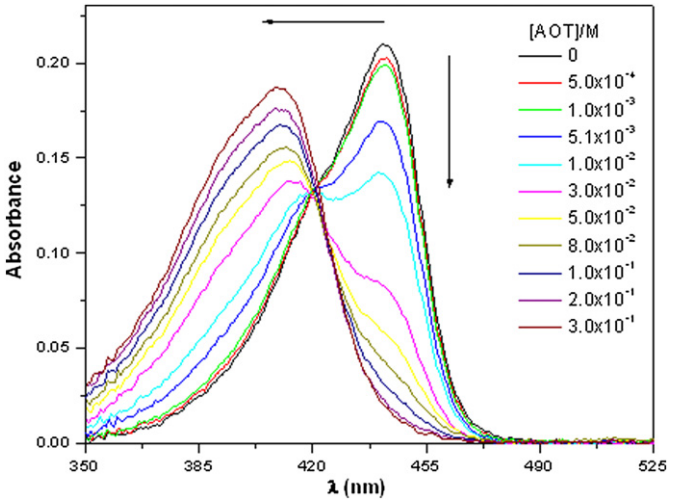

Fig. 1. Absorption spectra of C343 in benzene/AOT reverse micelles varying the [AOT] at $W_0 = 0$, [C343] = 6.0×10^{-6} M.

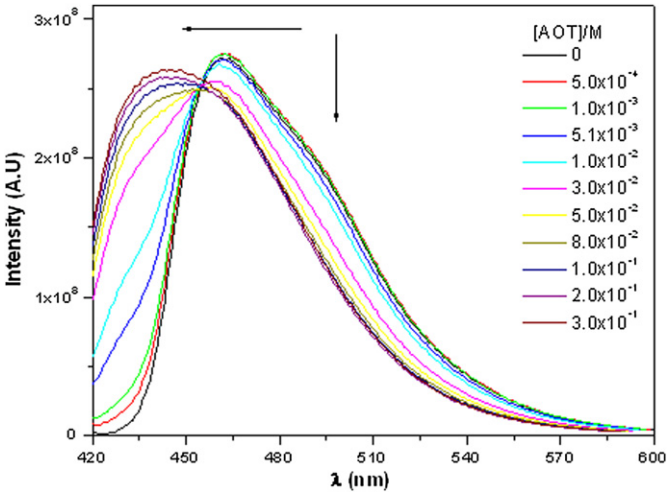

Fig. 2. Emission spectra of C343 in benzene/AOT RMs varying the [AOT] at $W_0 = 0$. [C343] = 6.0×10^{-6} M. $\lambda_{exc} = 418$ nm.

spectra of C343 in benzene/AOT RMs varying the AOT concentration. It can be seen that until [AOT] = 0.01 M, there is practically no variation on the C343 emission maxima that corresponds to the dimer species ($\lambda_{maxem} = 462$ nm). After that, the band shifts hypsochromically to $\lambda_{maxem} = 444$ nm which is characteristic of the C343 monomer located at the RMs' interface [10].

3.1.1. Calculation procedure of the molecular probe partition constant

The partition of C343 between AOT RMs and the external solvent, benzene, was treated within the framework of the pseudophase model [34,36–41]. This model considers the RMs as a distinct pseudophase whose properties are independent of the surfactant concentration and are only determined by the value of the characteristic parameter W_0. In this model, only two solubilization sites are considered, that is, the external solvent and the RM interface (i.e. all the surfactant molecules). In this way, the distribution of C343 between the micelles and the external solvent pseudophase defined in Eq. (3) can be expressed in terms of the partition constant K_p shown in Eq. (4):

$$C343_f \rightleftharpoons C343_b^{\#} \tag{3}$$

$$K_p = \frac{[C343]_b^{\#}}{[C343]_f} \tag{4}$$

The terms in brackets represent free (f) and bound (b) C343, in terms of local concentrations. If $[C343]_b$ is the analytical (bulk) concentration of micelle bound substrate, Eq. (5) holds.

$$[C343]_b\# = \frac{[C343]_b}{[AOT]} \tag{5}$$

and hence K_p can be expressed as in Eq. (6)

$$K_p = \frac{[C343]_b}{[C343]_f[AOT]} \tag{6}$$

where $[C343]_f$ is the concentration of the substrate in the organic solvent, and [AOT] is the AOT concentration. This equation applies at a fixed value of W_0 and when $[C343]_T \ll [AOT]$ where $[C343]_T$ is the probe analytical concentration.

The values of K_p can be determined from the changes with the surfactant concentration at a given W_0 in the C343 absorption spectra (Fig. 1) measured at a given wavelength. Thus, for C343 K_p was determined using Eq (7) [42–44].

$$A^{\lambda} = \frac{\left(\varepsilon^f + \varepsilon^b[AOT]K_p\right)[C343]_T}{(1 + K_p[AOT])} \tag{7}$$

where A^{λ} is the absorbance at different surfactant concentration, ε^f and ε^b are the molar extinction coefficients for C343 in benzene and in AOT RMs' interface, respectively, and $[C343]_T$ is the total dye concentration.

Fig. 3 shows representative plots of C343 absorption maxima at $\lambda = 451$ nm as a function of AOT concentration at $W_0 = 0$. Also, the data at [AOT] = 0 that correspond to C343 in pure benzene is plotted for comparison. The data shown in the figure were fitted to Eq. (7) using a non-linear regression method and the K_p values obtained is $73 \pm 5\ M^{-1}$.

3.2. C343 in benzene/AOT/water reverse micelles. $W_0 = 10$

With the addition of water to the AOT RMs, the C343 spectra change in comparison with the system with no water addition ($W_0 = 0$). Fig. 4A shows absorption spectra of C343 as a function of

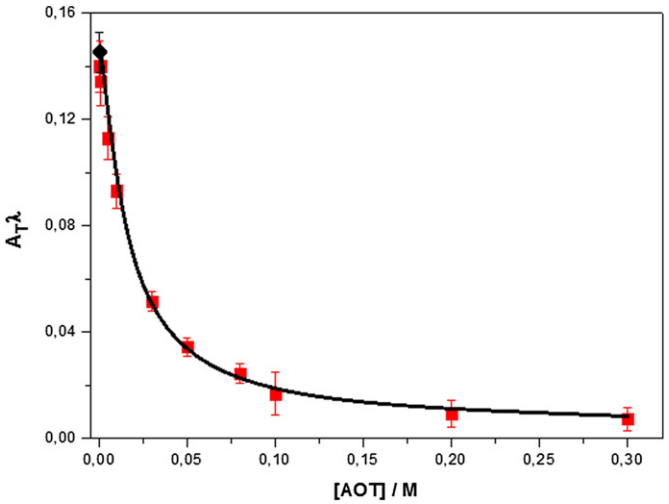

Fig. 3. C343 absorbance changes (From Fig. 1 at $\lambda = 451$ nm) with the surfactant concentration for benzene/AOT RMs at $W_0 = 0$. $[C343] = 6.0 \times 10^{-6}$ M. The black line is the fitting of the data to Eq. (7). ◆ Corresponds to C343 absorbance value in pure benzene.

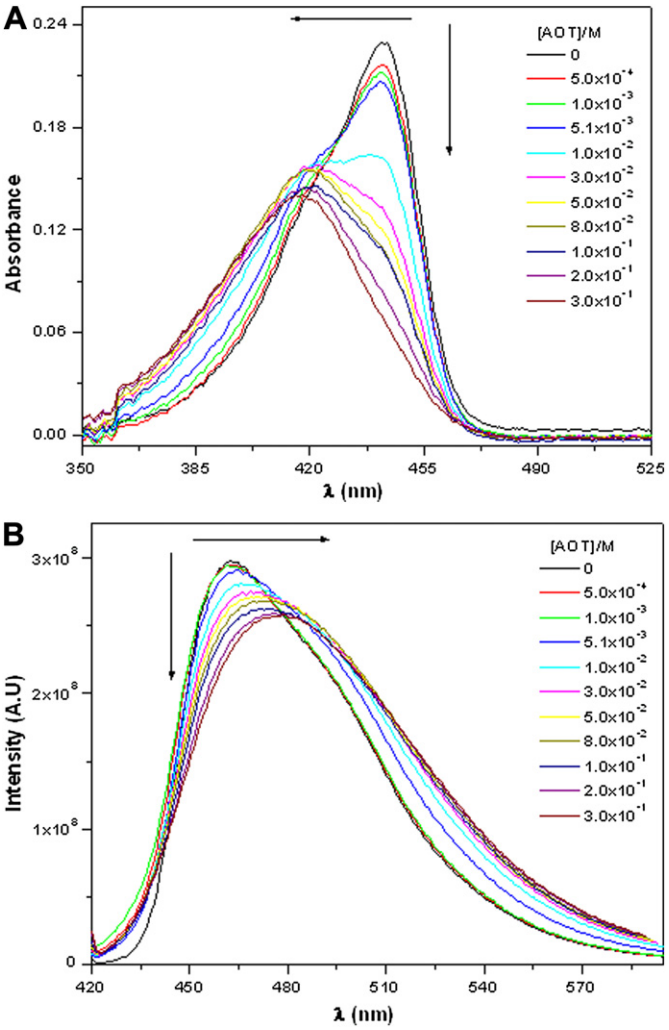

Fig. 4. (A) Absorption spectra of C343 in benzene/AOT/water reverse micelles varying the [AOT] at $W_0 = 10$. (B) Emission spectra of C343 in benzene/AOT/water reverse micelles varying the [AOT] at $W_0 = 10$, $[C343] = 6.0 \times 10^{-6}$ M. $\lambda_{exc} = 418$ nm.

[AOT] at $W_0 = 10$ while Fig. 4B shows the emission spectra of C343 in benzene/AOT/water RMs varying the AOT concentration at $\lambda_{exc} = 418$ nm. As it can be observed, the absorption spectra of C343 shows the absorption maxima characteristic of the dimer ($\lambda_{max} = 442$ nm) at low [AOT], while at surfactant concentration higher than 5.1×10^{-3} M the dimer band develops to the monomer species band located at $\lambda_{max} = 417$ nm at any surfactant concentration. It should be noted that the monomer band peaks 8 nm to lower energy in comparison with the monomer absorption band at $W_0 = 0$ which reflects the fact that the micropolarity of the RMs' interface increases in the presence of water [10].

Fig. 5 shows the changes in the λ_{maxem} values for C343 in benzene/AOT/water RMs at $W_0 = 10$ varying the surfactant concentration at $\lambda_{exc} = 418$ nm. Also, the data at [AOT] = 0 that correspond to C343 in pure benzene (without water addition) is plotted for comparison. From Figs. 4B and 5 it can be seen that the behavior of C343 is different at $W_0 = 10$ in comparison with $W_0 = 0$ (Fig. 2) because of, upon the water addition, the emission band shifts bathochromically as the surfactant concentration increases. It moves from $\lambda_{max} = 462$ nm (characteristic of the dimer in benzene) to $\lambda_{max} = 478$ nm at [AOT] greater than 0.10 M. It seems that, C343 monomer after excitation senses a polar environment at the AOT RMs' interface due to the presence of water molecules [28]. It must be noted that in benzene/AOT/water RMs the micropolarity sensed by C343 at the interface is greater than the one observed in *n*-heptane/AOT/water RMs [10]. It seems that water molecules penetrate more into the oil side of the RMs' interface when benzene is the non-polar organic solvent as it was suggested previously [28–31].

In summary, as we only detect the C343 monomer species in benzene/AOT RMs without and with water we expect that C343 exists at the RM interface, with the carboxylic end of the molecule pointing toward the polar head of the surfactant. In this non-polar environment the C343 intramolecular H-bond is reinforced and the carboxylic proton is not available to interact with the polar head of AOT.

From the inflection point of the plot presented in Fig. 6, the CMC value can be determined giving a value of around 2.5×10^{-2} M at $W = 0$ (not shown) and 7.3×10^{-3} M at $W_0 = 10$, similar to previous result for benzene/AOT RMs at W_0 [45]. Since it is known that for RMs the CMC values depend on the method used to determine it, it is customary to define this concentration value as *operational* CMC

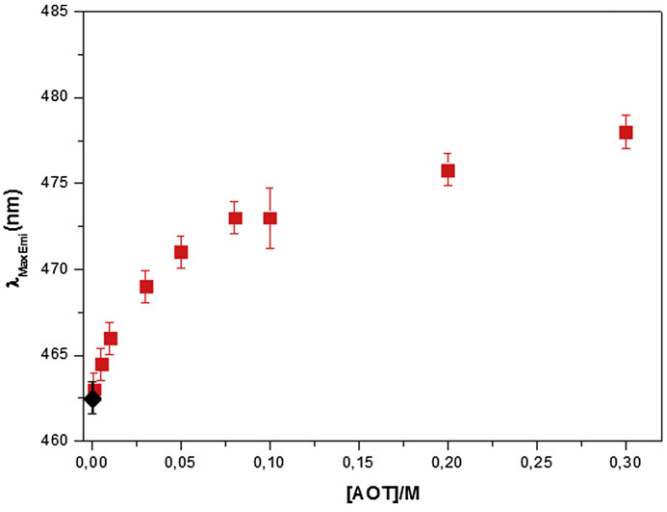

Fig. 5. Emission maxima shifts of C343 in benzene/AOT/water reverse micelles varying [AOT] at $W_0 = 10$. ◆ Corresponds to C343 emission maxima wavelength value in pure benzene. $\lambda_{exc} = 418$ nm.

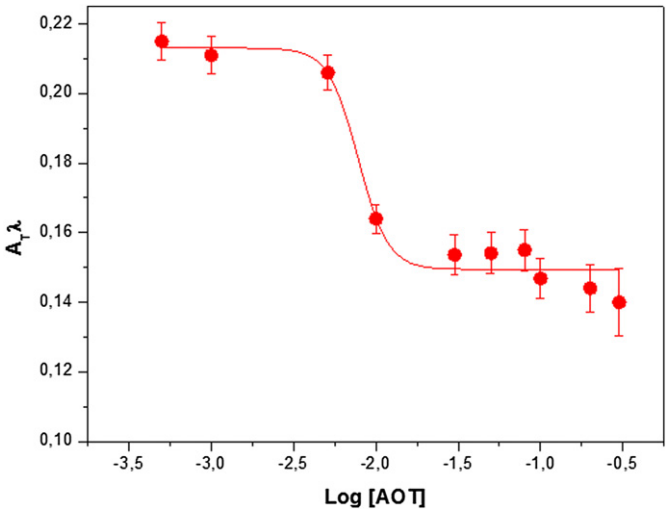

Fig. 6. Absorption values at 442 nm as a function of log [AOT], in benzene/AOT/water reverse micelles media at $W_0 = 10$. $[C343] = 6.0 \times 10^{-6}$ M.

[26,46,47]. As it was previously demonstrated for AOT the presence of water helps the RM formation with the consequent decreases in the CMC value [19,46]. Moreover, the results show the importance of the RMs' interface in the de-aggregation process of a dye and how this process can be used in order to determine a micellar parameter like CMC.

As it was discussed, at $W_0 = 0$, from the plot of C343 absorption maxima at $\lambda = 451$ nm as a function of AOT concentration at $W_0 = 10$ (results not shown) the K_p value was obtained. The data were fitted to Eq. (7) using a non-linear regression method and, the K_p values obtained is 62 ± 8 M^{-1}. As it can be observed the K_p values are similar at both W_0 investigated which is probably reflecting the fact that the dimer to monomer conversion has a crucial role in C343 partition process even more than the differences in the micropolarity.

4. Conclusion

We have performed a detailed study of the spectroscopy of coumarin 343 (C343), a common molecular probe, in benzene/AOT/water RMs. In the present contribution and because of the dye is soluble in pure benzene, for the first time using C343 as molecular probe it was possible to investigate the effect that the RM formation has on C343 spectroscopy.

Dissolved in pure benzene C343 exists in its dimeric form because of the strong intermolecular H-bond interaction. When introduced to the AOT RMs, C343 resides in the RMs' interface and, because of the low reverse micelles occupation number the probability of having more than one C343 molecule is dramatically reduced and only C343 monomer species is detected. From the spectral changes it was possible to determine the critical micelle concentration at $W_0 = 0$ and 10 and the C343 partition constants between two pseudophases. With regard to AOT RMs' interfacial properties it was demonstrated that water penetrates more to the oil side of the interface in comparison with *n*-alkanes/AOT RMs.

In summary, we demonstrated the importance of understanding the chemistry of molecular probes in homogeneous media in order to not introduce artifacts into the interpretation of the behavior in more complex media such as reverse micelles. Also, it has been shown, for the first time, the spectroscopic changes that C343 experiments due to the partition process that the dye undergoes because of the RMs' formation. Thus, our work reveals the

importance that the medium has on the behavior of a widespread dye used as chromophore, C343, for very different systems such as homogenous and microheterogenous media. We want to call the attention that considerable care in choosing and characterizing the molecular probe is required in order to analyze the results fully, especially if the dye can undergo a partition process between different pseudophases.

Acknowledgements

We gratefully acknowledge the financial support for this work by the Consejo Nacional de Investigaciones Científicas y Técnicas (CONICET), Agencia Córdoba Ciencia, Agencia Nacional de Promoción Científica y Técnica and Secretaría de Ciencia y Técnica de la Universidad Nacional de Río Cuarto. N.M.C., J.J.S. and R.D.F. hold a research position at CONICET. J.A.G thanks CONICET for a research fellowship.

References

[1] Schäfer EP. Dye lasers. 3rd ed. Berlin: Springer-Verlag; 1990.
[2] Riter RE, Undiks EP, Kimmel JR, Levinger NE. Formamide in reverse micelles: restricted environment effects on molecular motion. J Phys Chem B 1998;102:7931–8.
[3] Riter RE, Kimmel JR, Undiks EP, Levinger NE. Novel reverse micelles partitioning nonaqueous polar solvents in a hydrocarbon continuous phase. J Phys Chem B 1997;101:8292–7.
[4] Riter RE, Undiks EP, Levinger NE. Impact of counterion on water motion in aerosol ot reverse micelles. J Am Chem Soc 1998;120:6062–7.
[5] Willard DM, Riter RE, Levinger NE. Dynamics of polar solvation in lecithin/water/cyclohexane reverse micelles. J Am Chem Soc 1998;120:4151–60.
[6] Singh PK, Kumbhakar M, Pal H, Nath S. Modulation in the solute location in block copolymer–surfactant supramolecular assembly: a time-resolved fluorescence study. J Phys Chem B 2009;113:1353–9.
[7] Denat F, Diaz-Fernandez YA, Pasotti L, Sok N, Pallavicini P. A micellar multitasking device: sensing ph windows and gauging the lipophilicity of drugs with fluorescent signals. Chem Eur J 2009;16:1289–95.
[8] Singh PK, Kumbhakar M, Ganguly R, Aswal VK, Pal H, Nath S. Time-resolved fluorescence and small angle neutron scattering study in pluronics–surfactant supramolecular assemblies. J Phys Chem B 2010;114:3818–26.
[9] Riter RE, Willard DM, Levinger NE. Water immobilization at surfactant interfaces in reverse micelles. J Phys Chem B 1998;102:2705–14.
[10] Correa NM, Levinger NE. What can you learn from a molecular probe? New insights on the behavior of C343 in homogeneous solutions and AOT reverse micelles. J Phys Chem B 2006;110:13050–61.
[11] Cave JR, Castner Jr EW. Time-dependent density functional theory investigation of the ground and excited states of coumarins 102, 152, 153, and 343. J Phys Chem A 2002;106:12117–23.
[12] Drexhage KH, Eikson GR, Hawks GH, Reynolds GA. Water-soluble coumarin dyes for flashlamp-pumped dye lasers. Opt Commun 1975;15:399–403.
[13] Pant D, Levinger NE. Polar solvation dynamics in nonionic reverse micelles and model polymer solutions. Langmuir 2000;16:10123–30.
[14] Corbeil EM, Levinger NE. Dynamics of polar solvation in quaternary microemulsions. Langmuir 2003;19:7264–70.
[15] Pant D, Girault HH. Time-resolved total internal reflection fluorescence spectroscopy, Part I. Photophysics of Coumarin 343 at liquid/liquid interface. Phys Chem Chem Phys 2005;7:3457–63.
[16] Pant D, Le Guennec M, Illien B, Girault HH. The pH dependent adsorption of Coumarin 343 at the water/dichloroethane interface. Phys Chem Chem Phys 2004;6:3140–6.
[17] Yamasaki T, Kajimoto O, Hara K. High-pressure studies on AOT reverse micelar aggregate by fluorescence probe method. J Photochem Photobiol A: Chem 2003;156:145–50.
[18] Gutierrez JA, Falcone RD, Silber JJ, Correa NM. Role of the medium on the c343 inter/intramolecular hydrogen bond interactions. An absorption, emission, and ^{1}H NMR investigation of C343 in benzene/*n*-heptane mixtures. J Phys Chem A 2010;114:7326–30.
[19] Silber JJ, Biasutti MA, Abuin E, Lissi E. Interactions of small molecules with reverse micelles. Adv Colloid Interface Sci 1999;82:189–252.
[20] De TK, Maitra A. Solution behaviour of aerosol OT in non-polar solvents. Adv Colloid Interface Sci 1995;59:95–193.
[21] Moulik SP, Paul BK. Structure, dynamics and transport properties of microemulsions. Adv Colloid Interface Sci 1998;78:99–195.
[22] Hazra P, Chakrabarty D, Sarkar N. Intramolecular charge transfer and solvation dynamics of coumarin 152 in aerosol-OT, water-solubilizing reverse micelles, and polar organic solvent solubilizing reverse micelles. Langmuir 2002;18:7872–9.
[23] Imai AUM, Suzuki I. The most favorable condition for lipid hydrolysis by *Rhizopus delemar* lipase in combination with a sugar-ester and alcohol W/O microemulsion system. Colloids Surf A: Physicochem Eng Aspects 2008;324:79–85.
[24] Satpati AK, Kumbhakar M, Nath S, Pal H. Influence of confined water on the photophysics of dissolved solutes in reverse micelles. Chem Phys Chem 2009;10:2966–78.
[25] Agazzi FM, Falcone RD, Silber JJ, Correa NM. Solvent blends can control cationic reversed micellar interdroplet interactions. The effect of *n*-heptane:benzene mixture on bhdc reversed micellar interfacial properties: droplet sizes and micropolarity. J Phys Chem B 2011;115:12076–84.
[26] Falcone RD, Correa NM, Biasutti MA, Silber JJ. Properties of AOT aqueous and nonaqueous microemulsions sensed by optical molecular probes. Langmuir 2000;16:3070–6.
[27] Silva FO, Fernández MA, Silber JJ, De Rossi RH, Correa NM. Inhibited phenol ionization in reverse micelles: confinement effect at the nanometer scale. ChemPhysChem 2012;13:124–30.
[28] Correa NM, Biasutti MA, Silber JJ. Micropolarity of reverse micelles of aerosol-OT in *n*-hexane. J Colloid Interface Sci 1995;172:71–6.
[29] Mukerjee K, Moulik SP, Mukherjee DP. Thermodynamics of micellization of Aerosol OT in polar and nonpolar solvents. A calorimetric study. Langmuir 1993;9:1727–30.
[30] Ueda M, Schelly ZA. Controlled partial pressure–vapor pressure osmometry (CPP–VPO): a new method for the characterization of reverse micelles and WO microemulsions. J Colloid Interface Sci 1988;124:673–6.
[31] Heatley F. A ^{1}H nuclear magnetic resonance chemical-shift study of inverted microemulsions of aerosol OT in benzene and cyclohexane. Partitioning of water between hydrocarbon and aqueous phases. J Chem Soc Faraday Trans 1988;84:343–54.
[32] Lang J, Jada A, Mallaris A. Structure and dynamics of water-in-oil droplets stabilized by sodium bis(2-ethylhexyl)sulfosuccinato. J Phys Chem 1988;92:1946–53.
[33] Maiti NC, Mazumdar S, Periasamy N. J- and H-aggregates of porphyrin–surfactant complexes: time-resolved fluorescence and other spectroscopic studies. J Phys Chem B 1998;102:1528–38.
[34] (a) Falcone RD, Correa NM, Biasutti MA, Silber JJ. Acid–base and aggregation processes of acridine orange base in *n*-heptane/AOT/water reverse micelles. Langmuir 2002;18:2039–47;
(b) Molina PG, Silber JJ, Correa NM, Sereno LE. Electrochemistry in AOT reverse micelles. A powerful technique to characterize organized media. J Phys Chem C 2007;111:4269–76.
[35] Togashi DM, Costa SMB, Sobral AJFN, Gonsalves AMd'AR. Self-aggregation of lipophilic porphyrins in reverse micelles of aerosol OT. J Phys Chem B 2004;108:11344–56.
[36] Silber JJ, Falcone RD, Correa NM, Biasutti MA, Abuin E, Lissi E, et al. Exploratory study of the effect of polar solvents upon the partitioning of solutes in nonaqueous reverse micellar solutions. Langmuir 2003;19:2067–71.
[37] Lissi E, Engel T. Incorporation of n-alkanols in reverse micelles in the AOT/*n*-heptane/water system. Langmuir 1992;8:452–5.
[38] Rubio MA, Lissi EA. Photooxidation of anthracene derivatives in AOT/heptane reversed micelles. J Colloid Interface Sci 1989;128:458–63.
[39] Encinas MV, Lissi E. Solubilization of neutral molecules in AOT inverse micelles in *n*-heptane. Chem Phys Lett 1986;132:545–8.
[40] Aguilar LF, Abuin E, Lissi E. A procedure for the joint evaluation of substrate partitioning and kinetic parameters for reactions catalyzed by enzymes in reverse micellar solutions: I. Hydrolysis of 2-naphthyl acetate catalyzed by lipase in sodium 1,4-bis(2-ethylhexyl) sulfosuccinate (AOT)/buffer/heptane. Arch Biochem Biophys 2001;388:231–6.
[41] Falcone RD, Biasutti MA, Correa NM, Silber JJ, Lissi E, Abuin E. Effect of the addition of a nonaqueous polar solvent (glycerol) on enzymatic catalysis in reverse micelles. Hydrolysis of 2-naphthyl acetate by α-chymotrypsin. Langmuir 2004;20:5732–7.
[42] Correa NM, Zorzan DH, Chiarini M, Cerichelli G. Reverse micellar aggregates: effect on ketone reduction. 1. Substrate role. J Org Chem 2004;69:8224–30.
[43] Correa NM, Zorzan DH, D'Anteo L, Lasta E, Chiarini M, Cerichelli G. Reverse micellar aggregates: effect on ketone reduction. 2. Surfactant role. J Org Chem 2004;69:8231–8.
[44] Novaira M, Moyano F, Biasutti MA, Silber JJ, Correa NM. An example of how to use AOT reverse micelle interfaces to control a photoinduced intramolecular charge-transfer process. Langmuir 2008;24:4637–46.
[45] Ueda M, Schelly ZA. Reverse micelles of aerosol-OT in benzene. 4. Investigation of the micropolarity using 1-methyl-8-oxyquinolinium betaine as a probe. Langmuir 1989;5:1005–8.
[46] Correa NM, Biasutti MA, Silber JJ. Micropolarity of reversed micelles: comparison between anionic, cationic, and nonionic reversed micelles. J Colloid Interface Sci 1996;184:570–8.
[47] Novaira M, Biasutti MA, Silber JJ, Correa NM. New Insights on the photophysical behavior of prodan in anionic and cationic reverse micelles: from which state or states does it emit? J Phys Chem B 2007;111:748–59.